

## Preparation and Investigation of TiO<sub>2</sub>, SnS<sub>x</sub>, and SnO<sub>2</sub> Thin Film Properties for Use as UV Detectors

N. H. Bader\*, S. J. Kasim

Physics Department, Collage of Science, University of Basrah, Basrah, Iraq

\*Corresponding author E-mail: [noorhassanbader.88@gmail.com](mailto:noorhassanbader.88@gmail.com)

Doi:10.29072/basjs.20220212

<b>ARTICLE INFO</b>	<b>ABSTRACT</b>
<p><b>Keywords</b></p> <p>Hydrothermal, TiO<sub>2</sub>, SnO<sub>2</sub>, UV detector</p>	<p>Hydrothermal method was used to prepare TiO<sub>2</sub> films at temperatures (150,160,170,180)°C with a holding time of 6h, and the SILAR method was used to prepare the SnS<sub>x</sub> film. Through XRD assays, the shape of the TiO<sub>2</sub> compound is quaternary rutile in all samples and has a preferred growth direction towards (101), and we note that when the temperature increases, the intensity of the peaks decreases. XRD assays confirmed that the samples prepared by the SILAR method confirmed that the compound SnS<sub>x</sub> consists of the two compounds SnS and SnS<sub>2</sub>, as the compound SnS has a rhombic structure and the compound SnS<sub>2</sub> has a hexagonal shape. We note that all the manufactured FTO/TiO<sub>2</sub>/Al, FTO/n-TiO<sub>2</sub>/p-SnS<sub>x</sub>/Al, FTO/n-TiO<sub>2</sub>/p-SnO<sub>2</sub>/Al optical reagents have a nonlinear Schottky behavior. Al-TiO<sub>2</sub> reagents at different temperatures have a high sensitivity of about 9900%, and the sensitivity of the detector decreases with the increase in the applied voltage, and it has a slow response, so we dope it with materials SnS<sub>x</sub>, SnO<sub>2</sub>. As for the TiO<sub>2</sub>/SnS<sub>x</sub>, TiO<sub>2</sub>/SnO<sub>2</sub> reagents, we note that the highest sensitivity is 40400% for the FTO/n-TiO<sub>2</sub>/p-SnS<sub>x</sub>/Al detector with at a voltage of 0 V. Also, the sensitivity decreases with an increase in the applied voltage and its response is fast.</p>

Received 11 Jun 2022; Received in revised form 13 Aug 2022; Accepted 25 Aug 2022, Published 31 Aug 2022



## 1. Introduction

Nanotechnology is an active field of research with both new sciences and useful applications that have gradually established themselves in the past two decades. Nanotechnology is a term encompassing science, engineering and materials applications [1], which involves harnessing the unique physical, chemical, and biological properties of nanomaterials in fundamentally new and useful ways [2]. This emerging technology has many possible applications and therefore affects various technological fields including advanced materials, biotechnology, pharmacy, electronics, scientific instruments and industrial manufacturing processes. From a scientific point of view, nanotechnology can be defined as referring to materials and systems with structures and components that exhibit physical and chemical properties [3]. The use of UV detectors on a large scale in achieving the process of visible blindness, in the recent period, semiconductors with nanostructures such as nanosticks, nanowires, nanotubes, and nanostrands have attracted wide research interest due to their high surface-to-size ratio and surface conformation [4,5,6]. Nanostructured conductors Nuclei such as titanium dioxide ( $\text{TiO}_2$ ) are of much interest due to their photoelectric properties and remarkable catalytic activity [7]. The molecular formula for titanium dioxide is  $\text{TiO}_2$ .  $\text{TiO}_2$  has very high photocatalytic activities and is non-toxic, chemically stable, biocompatible and strong oxidizing agent (large surface area), it is a cheap material and low production cost. Thermodynamically polymorphic structures. Titanium dioxide ( $\text{TiO}_2$ ) is an important semiconductor material with a wide bandgap energy gap (3.02 eV and 3.20 eV for Rutile and Anatase respectively) and is an n-type semiconductor. On the other hand, tin sulfide is a semiconductor and  $\text{SnS}_x$  ( $x = 1,2$ ) compounds are non-toxic and low-cost,  $\text{SnS}_x$  materials have excellent chemical stability and reversibility due to their unique structure [8]. Tin sulfides have received great attention due to their structural diversity and containing several binary compounds such as  $\text{SnS}$ ,  $\text{Sn}_2\text{S}_3$ ,  $\text{Sn}_3\text{S}_4$ ,  $\text{Sn}_4\text{S}_5$ , and  $\text{SnS}_2$  [9, 10]. Among these compounds, tin monosulfide ( $\text{SnS}$ ) and tin disulfide ( $\text{SnS}_2$ ) are the most important and have received a lot of attention for their intriguing properties and many applications [10]. The use of inexpensive methods for preparing high-quality nanocomposites has attracted the attention of researchers and the hydrothermal method is one of the methods used for this purpose. This method is a process for preparing many forms of nanomaterials such as thin films with nanostructures through a heterogeneous reaction in the presence of aqueous solvents under high temperatures and pressures [11]. One of the advantages of this method is that it is an easy way to manufacture many nanomaterials, as well as the growth parameters can be changed such as growth time and temperature [12, 13]. Another



method for depositing nano films is the SILAR method, reaction and adsorption of a layer of ions. This method is used to deposit thin films of metal ions, and it is a simple method It is fast and convenient for the deposition of films of semiconductors, oxides, chalcogens and polymers [14]. This method is an upgraded version of the Chemical Bath Deposition (CBD) method, and because it does not need to work at high temperatures, it does not need expensive technology equipment [15].

## 2. Experimental

### 2.1 Preparation of TiO<sub>2</sub> nanorods

At first we prepare Titanium(IV) butoxide by placing 5 ml of TiCl<sub>4</sub> in a three-necked flask and 10 ml of [CH<sub>3</sub>CHOHCH<sub>2</sub>CH<sub>3</sub>]butanol in a separator funnel and then the Butanol was distilled at a drop rate every 2-3 seconds using a magnetic stirrer at TiCl<sub>4</sub> with stirring until the disappearance of fog In the three-necked flask, a yellow viscous liquid of Titanium (IV) butoxide appeared as in Figure 1. Then the FTO substrates were washed with water and detergent to get rid of suspended matter, the FTO bases were kept in diluted HCL for 5 minutes and then cleaned with Ultrasound apparatus using acetone, ethanol and propanol each for 10 min and then washed with distilled water respectively, TiO<sub>2</sub> nanorods are prepared by hydrothermal method FTO was immersed at an angle in a stainless steel autoclave containing a 50 ml Teflon vessel containing the solution Prepared by adding 15 ml of hydrochloric acid, 15 ml of distilled water and 0.5 ml of Titanium (IV) butoxide. The autoclave was placed at different temperatures, (150,160,170,180,190)°C for 6 hours in the oven, then the samples were cooled. and clean them with distilled water as shown in Fig. 2.

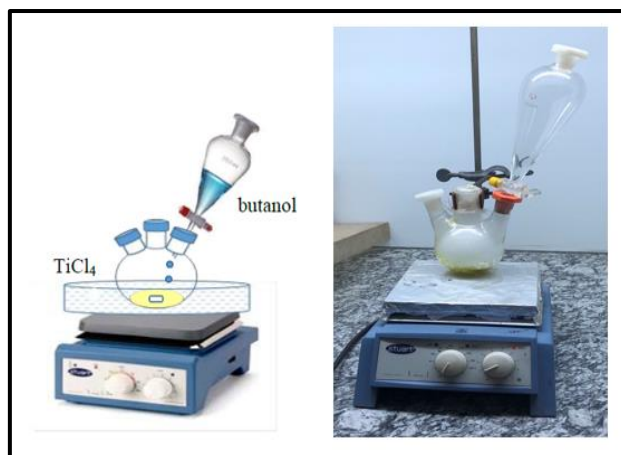


**Figure1:** Preparation of Titanium (IV) butoxid



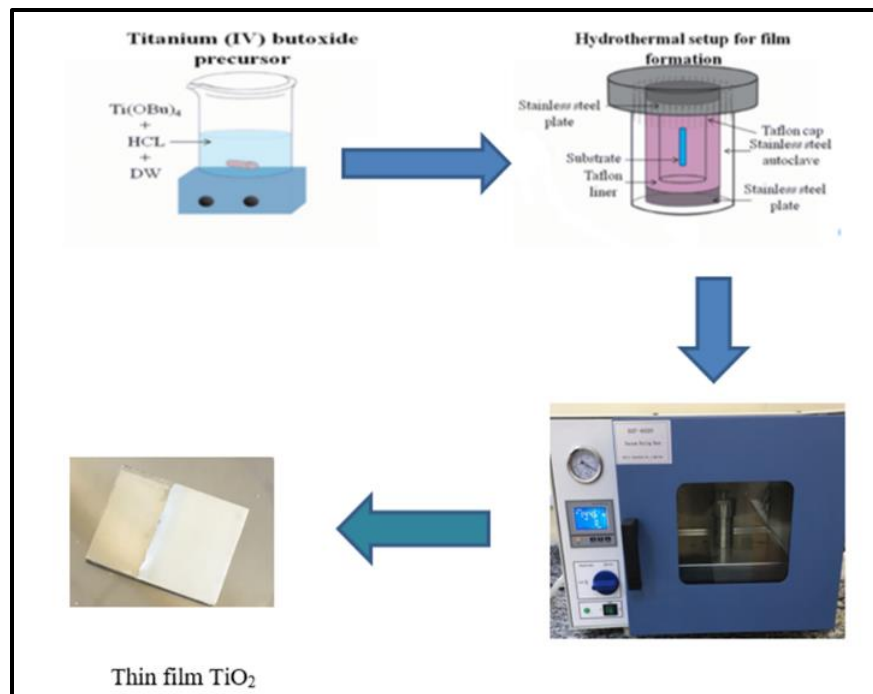


**Figure 2:** Steps of preparation TiO<sub>2</sub> nanorods

## 2.2 Preparation of Tin Sulfide SnS<sub>x</sub>

SnS<sub>x</sub> thin films were prepared by SILAR method by dissolving 0.2 M of SnCl<sub>2</sub>·2H<sub>2</sub>O in 50 ml of distilled water with 0.1M of Na<sub>2</sub>S in 50 ml of distilled water. The glass is then rinsed in distilled water for 10 seconds, then the glass is immersed in Na<sub>2</sub>S solution for 20 seconds, the sulfide ions react with the tin ions absorbed on the glass, and then it is rinsed in water for 10 seconds to remove impurities, thus one SILAR cycle is completed and after 125 cycles are completed. We obtained SnS<sub>x</sub> membranes and the experiment was conducted at room temperature as shown in Fig. 3a. When the SnS<sub>x</sub> film is annealed at a temperature of 400°C, it turns into a SnO<sub>2</sub> compound and its color changes to golden, as shown in Fig. 3b.

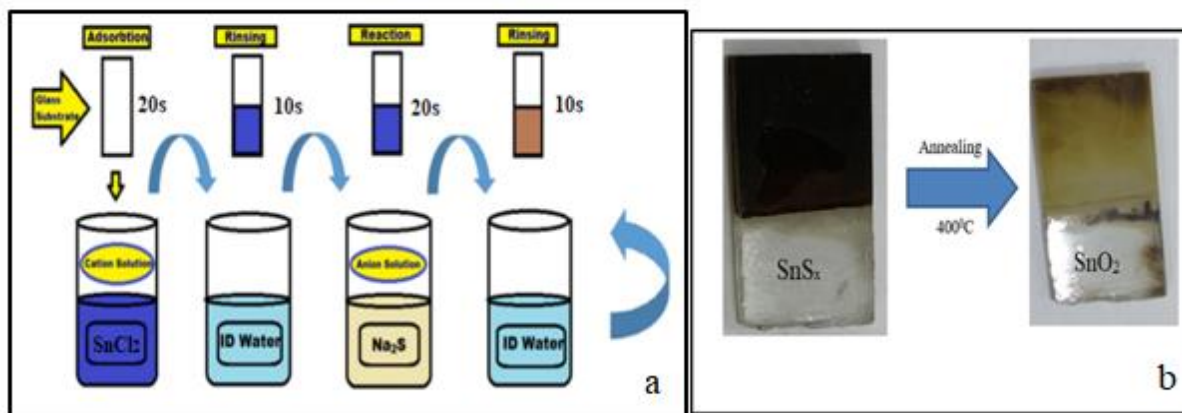


**Figure 3:** (a) Scheme for preparing SnS<sub>x</sub>, (b) Photographs of SnS<sub>x</sub> sample before annealing and SnO<sub>2</sub> after annealing

### 2.3 Fabrication of the Photodetector

The TiO<sub>2</sub>/SnS<sub>x</sub> photodiode was fabricated by depositing the SnS<sub>x</sub> films prepared by SILAR method on the thin TiO<sub>2</sub> films prepared on FTO substrates by the hydrothermal method, while the TiO<sub>2</sub>/SnO<sub>2</sub> photodiode is made by depositing the SnS<sub>x</sub> films prepared by the SILAR method on the thin TiO<sub>2</sub> films prepared on the TiO<sub>2</sub> thinner bases. At 400°C, its color turns golden, and then a layer of aluminum (Al) is deposited by thermal evaporation method on the surface of the SnS<sub>x</sub> films in the TiO<sub>2</sub>/SnS<sub>x</sub> duo and on the surface of the SnO<sub>2</sub> films. after annealing as shown in Fig.4. Then the connecting wires were attached to the FTO base and aluminum metal using Silver paste. The FTO substrate was used as the electrode with dimensions of 1.5 x 1cm, and the effective area of the photodetector manufactured was 1cm<sup>2</sup>.

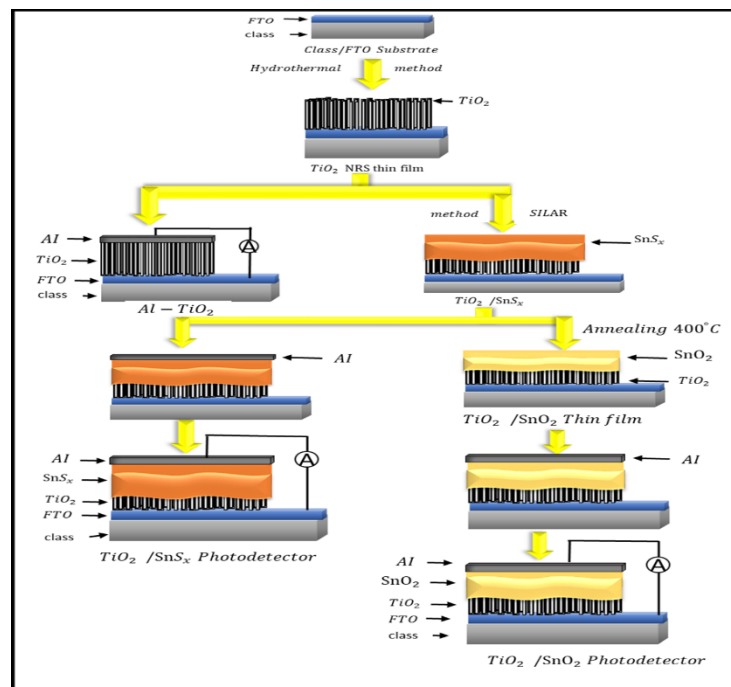


**Figure 4:** Schematic diagram of the manufactured reagents FTO/TiO<sub>2</sub>/Al, FTO/n-TiO<sub>2</sub>/p-SnO<sub>2</sub>/Al, FTO/ n-TiO<sub>2</sub>/p-SnO<sub>2</sub>/Al,

### 3. Results and discussion

#### 3.1 Structural analysis: X-ray diffraction

The structural properties of TiO<sub>2</sub> films prepared by hydrothermal method at different temperatures of 150,160,170,180, and 190°C were studied, and SnS<sub>x</sub> films prepared by SILAR method were prepared using X-ray diffraction technique and its diffraction pattern is shown in Fig. 5A where we notice the peaks (110), (101) (200), (211), (002) and (221) corresponding to the diffraction angles 2θ (26.69, 36.22, 37.93, 51.58, 62.94, 65.70) respectively at temperatures (150, 160, 170, 180)°C where the peaks (200), (211) belong to FTO and the other values belong to TiO<sub>2</sub> has a quaternary structure of a rutile type, and this result is consistent with (JCPDS 21-1272), but we note the preferred growth direction at (101) and at a temperature of 190°C. Furthermore, there are no peaks are appeared due to the increase in temperature, which causes rapid growth that leads to irregular formation The crystalline works on the peeling of the membrane where the crystal growth rate starts to decrease and as a result of these increases in the lengths of the rods leads to the breakage of the rods according to the results [13, 16]. The (c/a) approximate to the typical ratio of



the quaternary  $\text{TiO}_2$  compound and this result with (JCPDS 21-1272). Figure 5B shows the X-ray diffraction pattern without the film of the compound  $\text{SnS}_x$  prepared by SILAR method for 30 cycles. We notice the appearance of the first two peaks at (002) that belong to the compound  $\text{SnS}_2$  according to the card JCPDS (001-0687), while the other peak (201) belongs to the compound  $\text{SnS}$  according to the card JCPDS(73-1859), this shows that the prepared compound is  $\text{SnS}_x(x=1,2)$  which consists of two compounds,  $\text{SnS}_2, \text{SnS}$ .

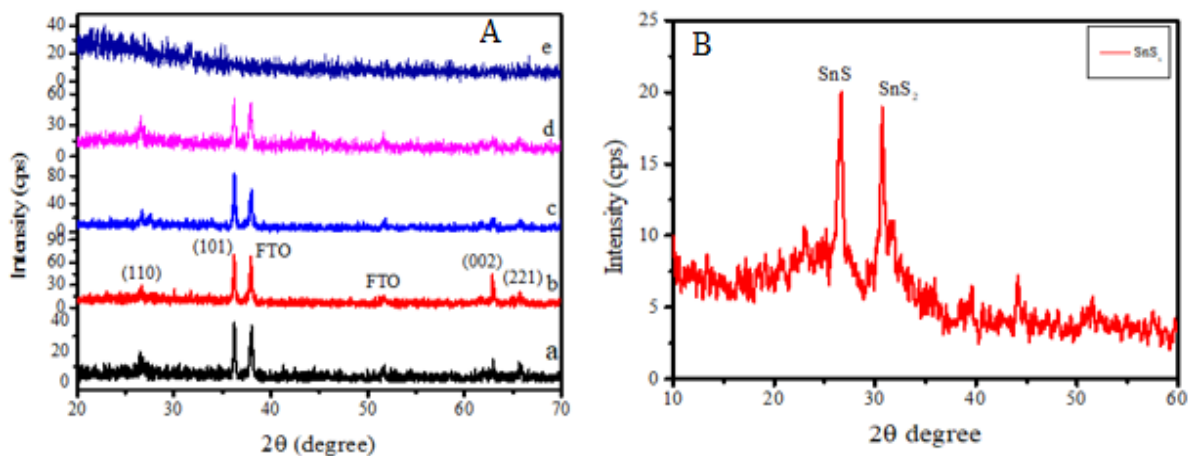


**Figure 5:** (A) X-ray diffraction pattern of  $\text{TiO}_2$  model prepared by hydrothermal method on FTO substrate at temperatures (a)150°C (b)160°C (c)170°C (d)180°C (e) 190°C,(B) X-ray diffraction pattern with no fading  $\text{SnS}_x$  prepared by SILAR method and with 30cycles

Table 1: The values of the lattice constants and particle size of the prepared samples

compound	G.S(nm)	c/a	c(nm)	a(nm)	Sample
Rutile	42.5	0.6468	2.9534	4.5656	150°C
	84.9	0.6428	2.9576	4.6009	160°C
	38.6	0.6467	2.9527	4.5652	170°C
	53.1	0.616	2.923	4.744	180°C

### 3.2 Surface Morphology properties

The surface properties of  $\text{TiO}_2$  films prepared by hydrothermal method were studied on FTO substrates at different temperatures 150°C, 160°C, and 170°C and  $\text{SnS}_x$  films prepared by SILAR



method. Rectangular and perpendicular to the base as shown in Fig. 6, and through the results that the size of the nanorods began to grow with the increase in the preparation temperature from 150°C to 170°C and continued to increase at a decreasing rate until the TiO<sub>2</sub> nanorods began to break at a high temperature about 180°C, where it begins to peel. As a result, it begins to degrade, which causes the membranes to peel off early, and this is consistent with [13, 16–19]. Using the Image J program, the average diameter of the nanorods was calculated, as it was observed that the diameter of the nanorods increased with increasing temperature, as the diameter of the nanorods at a temperature of 150°C (20-30) nm and a temperature of 160°C would be (30-40)nm, The temperature is 170°C and the diameter of the bars is (50-60)nm. Figure 7 shows FESEM images of SnS<sub>x</sub> films prepared by the SILAR method on glass bases with 30 cycles. We note from the figure that they are rod-shaped and the average diameter of the rods is (10-20) nm.



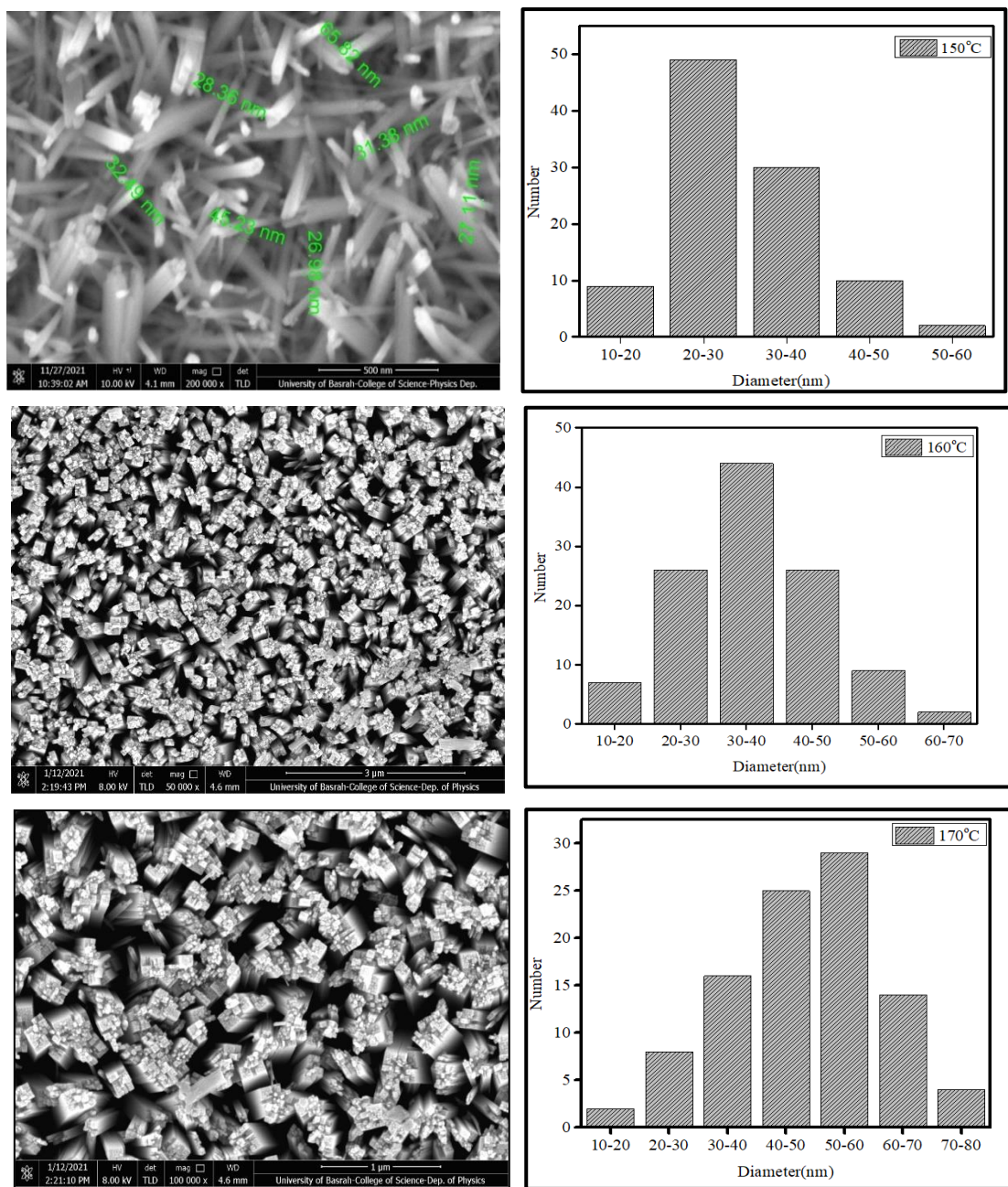


**Figure 6:** SEM and Diameter distribution of TiO<sub>2</sub> thin films at different temperatures

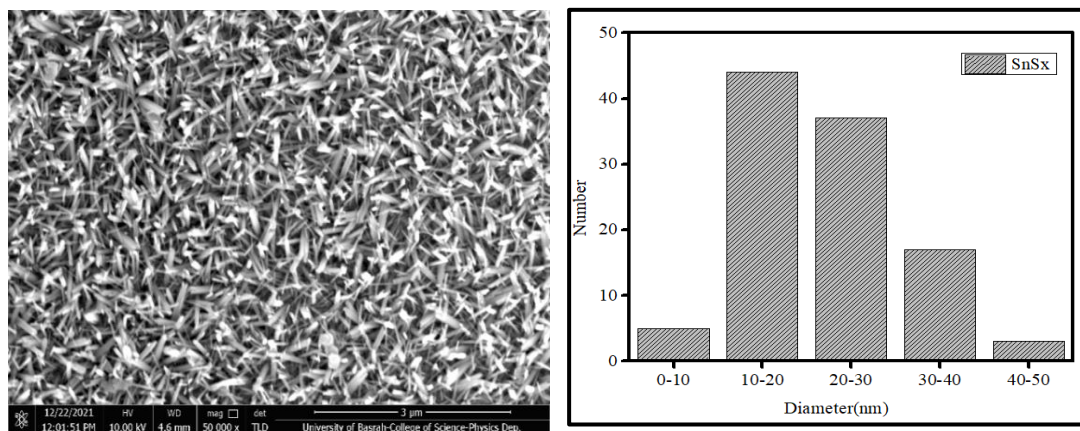


**Figure 7:** SEM and Diameter distribution of  $\text{SnS}_x$  thin films

### 3.3 Optical properties

The optical properties of the nanostructured thin films were studied using the absorption spectra of a wavelength range (300-1000). Figure 8 shows the absorption spectra of the films of the composite  $\text{TiO}_2$  prepared by the hydrothermal method and at different temperatures (150,160,170,180,190) $^\circ\text{C}$ , where they show strong absorption in the UV region between (300-400) nm and weak absorption in the visible region indicating that it has a wide energy gap and the absorbance increases with increasing temperature and at high temperatures the absorption was observed in the visible region  $\lambda > 410$  which is generally related to the absorption of visible light through surface defects  $\text{TiO}_2$  NRs and the energy gap was calculated. The  $E_g$  for films prepared using the absorbance spectrum from plot  $(\alpha h\nu)^2$  versus  $(h\nu)$  by extrapolating the straight-line curve to the photon energy axis intercept at  $((\alpha h\nu)^2 = 0)$  as shown in Fig. 9 which is consistent with the results [ 18–21]. We noted that there is little difference in the energy gap value. This difference is due to the difference in the size of the thin-film nanorod according to the increasing concentration and deposition temperature. The increase in crystallinity and regularity in the thin-film crystal structure may also be one of the reasons. In Fig.10, the absorption spectrum of the  $\text{SnS}_x$  films prepared by the SILAR method and 30 cycles on the bases of the glass and by annealing at a temperature of 400 $^\circ\text{C}$  turns into the compound  $\text{SnO}_2$ , where the absorption appears in the range (350-480) and the energy gap is calculated by extrapolating the straight line on the x-axis, which be consistent with research [22, 23].

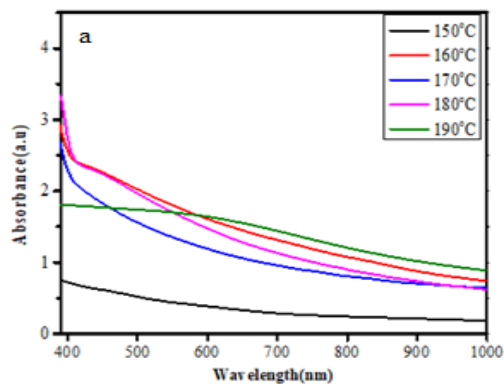


**Figure 8:** Absorption spectrum of TiO<sub>2</sub> films prepared by hydrothermal method on FTO substrate at different temperatures

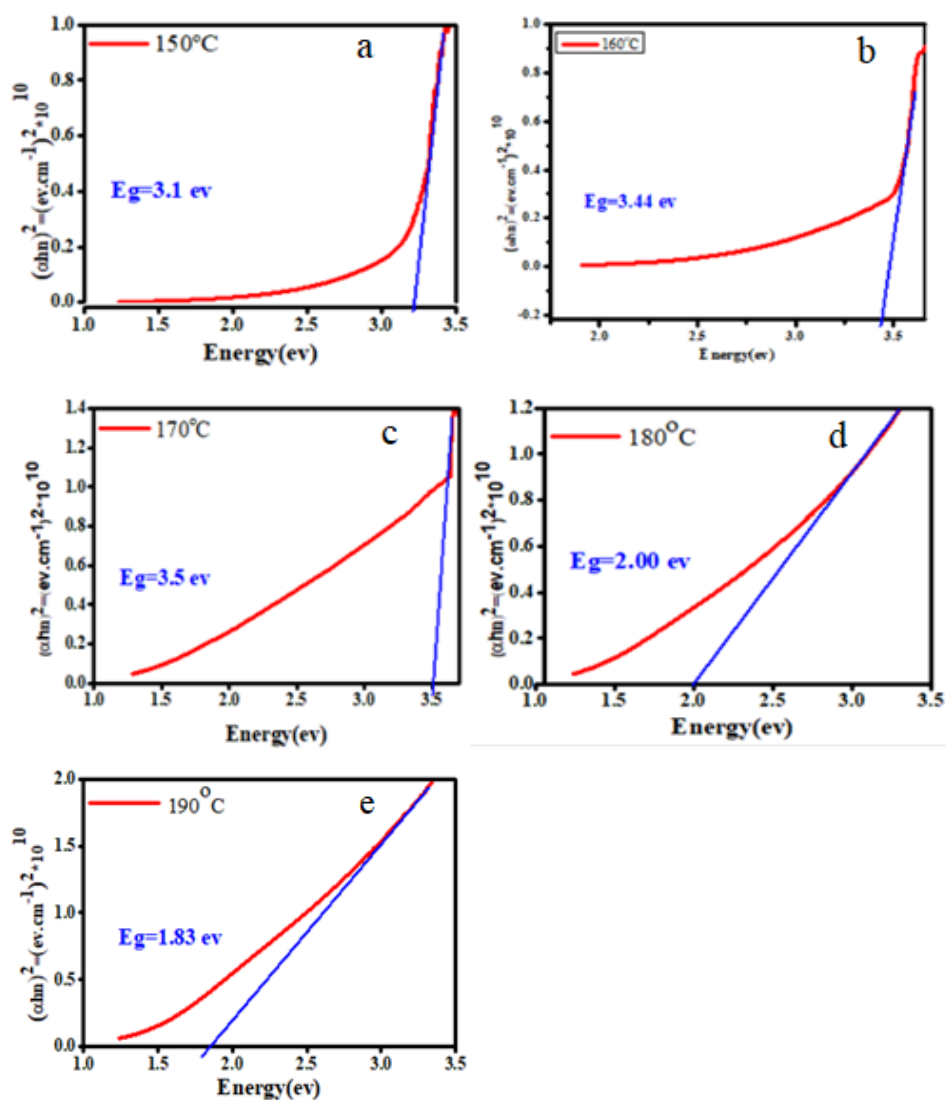


**Figure 9:** Energy gap values of TiO<sub>2</sub> films prepared by hydrothermal method on FTO substrates at different temperatures (a)150°C,(b)160°C,(c)170°C,(d)180°C,(e)190°C.



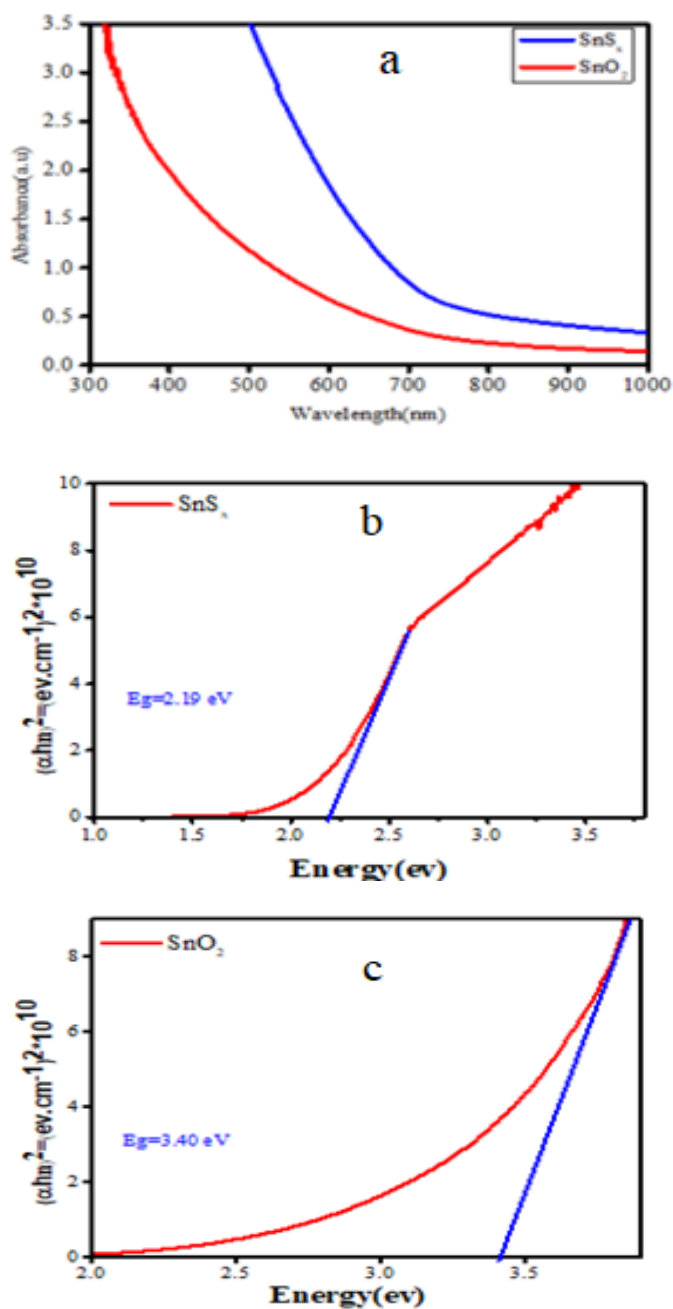


**Figure 10:** (a) Absorption spectrum of the films of the  $\text{SnS}_x$  prepared by SILAR method on glass bases at 30 cycles and of the  $\text{SnO}_2$  compound prepared from the heat treatment of  $\text{SnS}_x$  at  $400^\circ\text{C}$ , (b) Energy gap values for  $\text{SnS}_x$ , (c) Energy gap values for  $\text{SnO}_2$

Table 2: Energy gap values

substrate	compound	Eg(ev)	T(°C)
FTO	TiO <sub>2</sub>	3.1	150
		3.44	160
		3.5	170
	Rutile	2.00	180
		1.83	190
		2.53	160
		3.05	
		3.01	
Glass	SnS <sub>x</sub>	2.15	-----
	SnO <sub>2</sub>	3.40	----

### 3.4 Photoluminescence (PL)

Photoluminescence spectrum (PL) at room temperature for TiO<sub>2</sub> films prepared on FTO substrates by hydrothermal method at temperatures 150°C, 160°C using an excited wavelength of 325 nm. The spectra show an emission peak at 396 nm as shown in Figure 11. upon excitation with bandgap energy the photoexcited electrons relax to the lowest level of the excited state [24], that is, when TiO<sub>2</sub> is exposed to ultraviolet rays, its gap is recombined with the electron and emits light photons [25]. We observe a decrease in the intensity with increasing temperature and therefore the decrease in the intensity of the PL peak confirms the decrease in the recombination rate for electron gap pairs [26].



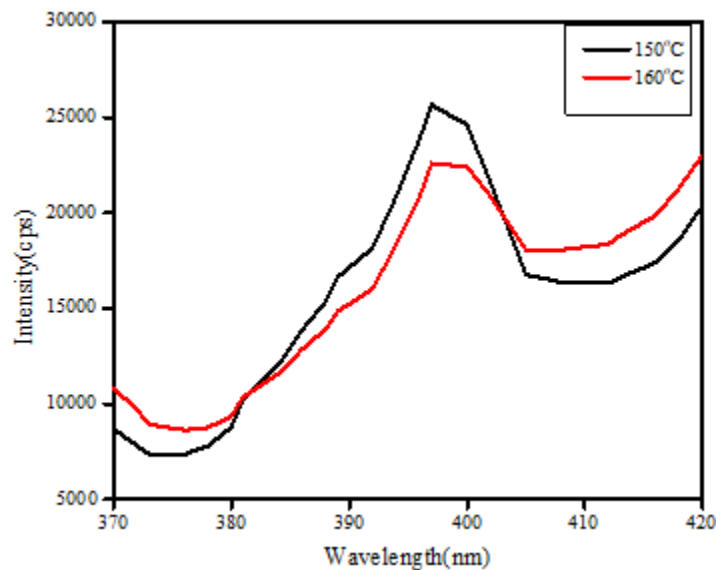


**Figure 11:** Photoluminescence spectra of TiO<sub>2</sub> films prepared by hydrothermal method at 150°C, 160°C.

### 3.5 Current-voltage Characteristics

The electrical properties of the photodetector in the dark and in the light were studied using Keithly 2400 device under applied forward and reverse bias voltage from -4 to +4 at room temperature. The figure shows 13a the change of the dark current as a function of the bias voltages applied to the two ends of the detector. The current increases linearly with the increase of the voltage applied to the membranes, meaning that the mechanical is non-ohmic. Figures 12,13, and 14 show the curves of the values of the current in the dark and the illumination passing through the detector as a function of the forward and reverse bias. In illumination, the detector was exposed to white light of intensity (0.67 mW/cm<sup>2</sup>). We note that all detectors show a non-linear (Schottky) behavior. In the forward bias, we notice a large increase in the value of the current with an increase in the applied voltage. The reason for the large increase in the current is due to the fact that the forward bias voltage will reduce the voltage barrier, that is, a decrease in the width of the depletion region, which leads to an increase in the speed of electrons. As for the reverse bias, the width of the depletion region will increase, which will lead to an obstruction in the movement of electrons, a large voltage barrier that works to straighten the current. We also note that the dark current is small, while the light current generated under illumination was high. In order to calculate the idealization factor ( $n$ ) by drawing the relationship between  $\ln I$  with the forward bias voltage in the dark state and the illumination at room temperature and from the slope of the straight line, the

idealization factor (n) can be calculated using Equation 1. As for calculating the voltage barrier height, the resulting saturation current  $I_0$  was calculated From the extension of the logarithmic curves of the current at its value ( $V = 0$ ) and from an equation 2, the height of the voltage barrier was calculated, as shown in Table 3.

$$n = \frac{q}{k_B T} \left( \frac{dv}{d(\ln(I))} \right) \tag{1}$$

$$\phi_b = \frac{k_B T}{q} = \ln \left( \frac{A A^* T^2}{I_0} \right) \tag{2}$$

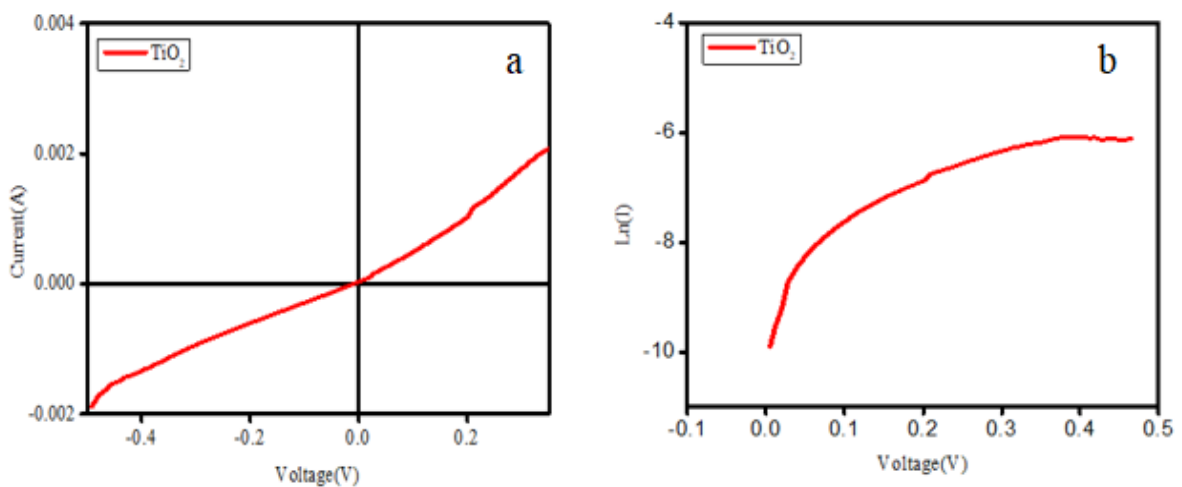


Figure 12: (a) Characteristic (I-V) for TiO<sub>2</sub> under darkness, (b) Ln(I) versus voltage (V)

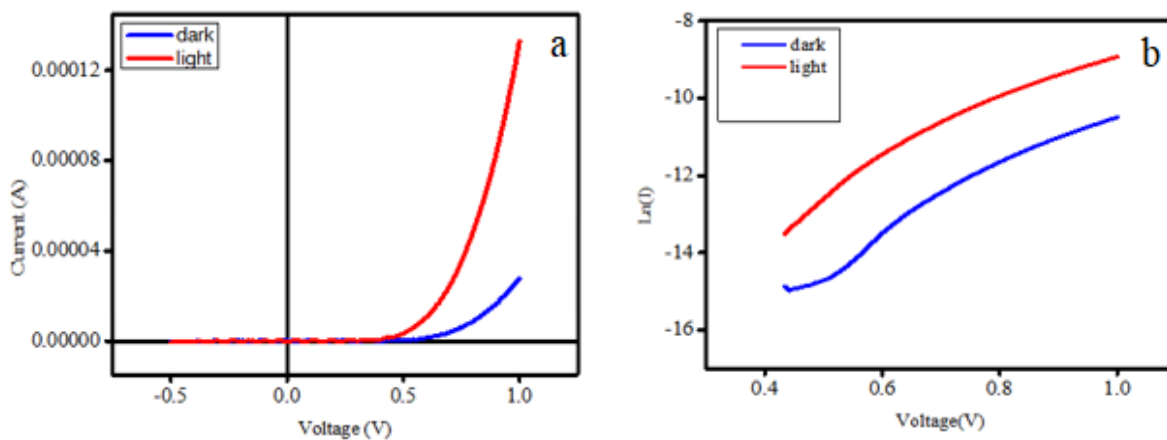


Figure 13: (a) Characteristic (I-V) Under Darkness and Illumination of the FTO/n-TiO<sub>2</sub>/p-SnS<sub>x</sub>/Al Detector, (b) Ln(I) versus voltage (V)



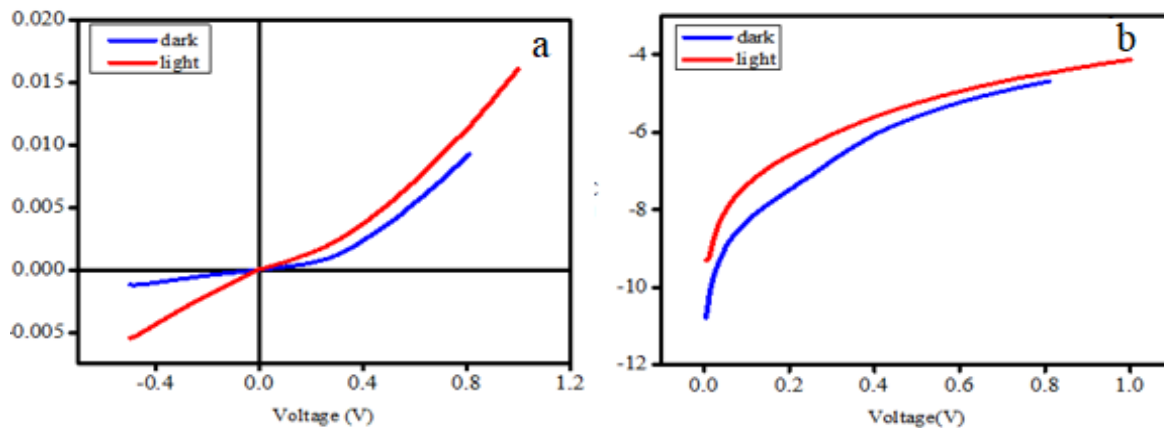


Figure 14: (a) Characteristic (I-V) Under Darkness and Illumination of the FTO/n-TiO<sub>2</sub>/p-SnO<sub>2</sub>/Al Detector, (b) Ln(I) versus voltage (V).

Table 3: values of the ideal factor, saturation current, and voltage barrier

Photodetector		TiO <sub>2</sub>	n-TiO <sub>2</sub> /p-SnS <sub>x</sub>	n-TiO <sub>2</sub> /p-SnO <sub>2</sub>
n	dark	6.154	4.452	7.673
I <sub>0</sub> (A)		3.562x10 <sup>-6</sup>	4.563x10 <sup>-7</sup>	1.165x10 <sup>-5</sup>
Φ <sub>B</sub> (eV)		0.684	0.827	0.773
n	Light	-----	4.980	7.437
I <sub>0</sub> (A)		-----	2.93x10 <sup>-6</sup>	1.224x10 <sup>-5</sup>
Φ <sub>B</sub> (eV)		-----	0.809	0.772



### 3.6 Photosensing properties

The optical sensing properties of the FTO/TiO<sub>2</sub>/Al detector as well as the n-TiO<sub>2</sub>/p-SnS<sub>x</sub>, n-TiO<sub>2</sub>/p-SnO<sub>2</sub> photodetectors prepared at different temperatures (150°C, 160°C, 170°C) were studied using ultraviolet light with a wavelength of 385nm and intensity of 0.05 mW. cm<sup>2</sup> at room temperature and by applying a different bias voltage. These rays were directed perpendicular to the photodetectors with a distance of (5 cm) and the response and sensitivity were calculated using the equations 3,4 respectively. The performance mechanism of photodiodes can be explained by the following steps: (1) generation of electron hole pairs by absorbing the incident light, (2) separation of electron hole pairs by the internal electric field of the junction and (3) current flowing in the external circuit to generate the output signal [27]. The rise time and the landing time were also calculated as shown in the table 3. The results obtained through the optical sensing properties of the FTO/TiO<sub>2</sub>/Al detector prepared by the hydrothermal method, at a temperature of 160°C, and for different bias voltages, as in the figure 14a. at 0V bias voltage, the light produces an electric field that gives an optical current and grows until it reaches saturation. The current increases from 0.001μA to 0.100μA by highlighting and it showed a high sensitivity of 9900%.

$$R_{\lambda} = \frac{I_{ph}}{P_{in}} \quad (3)$$

$$S = \frac{I_{ph} - I_d}{I_d} 100\% \quad (4)$$

We note from the results that when comparing the n-TiO<sub>2</sub>/p-SnS<sub>x</sub> reagents at different temperatures (150°C, 160°C, 170°C) at 0V, the photocurrent increases with increasing temperature, and the response is quick as the temperature increases, as shown in the figure 16d. As well as in the aforementioned detectors, the photocurrent increases with the increase in the applied voltage and the sensitivity decreases, as well as in the FTO/TiO<sub>2</sub>/Al detector the response is weak, but when a layer of SnS<sub>x</sub>, SnO<sub>2</sub> compounds is deposited, its response is fast and improves the performance of the photodetector as found in [20, 28]. It was observed in the FTO/n-TiO<sub>2</sub>/p-SnO<sub>2</sub>/Al FTO/n-TiO<sub>2</sub>/p-SnS<sub>x</sub>/Al reagents that the highest sensitivity is 40400% at a temperature of 170°C with a voltage of 0 V and a rise time of 0.17s with a drop time of 0.3s as well. Sensitivity decreases with increased voltage applied and its response is rapid. We note that the best reagent is FTO/n-TiO<sub>2</sub>/p-SnS<sub>x</sub>/Al as in the Fig. 15b,c.



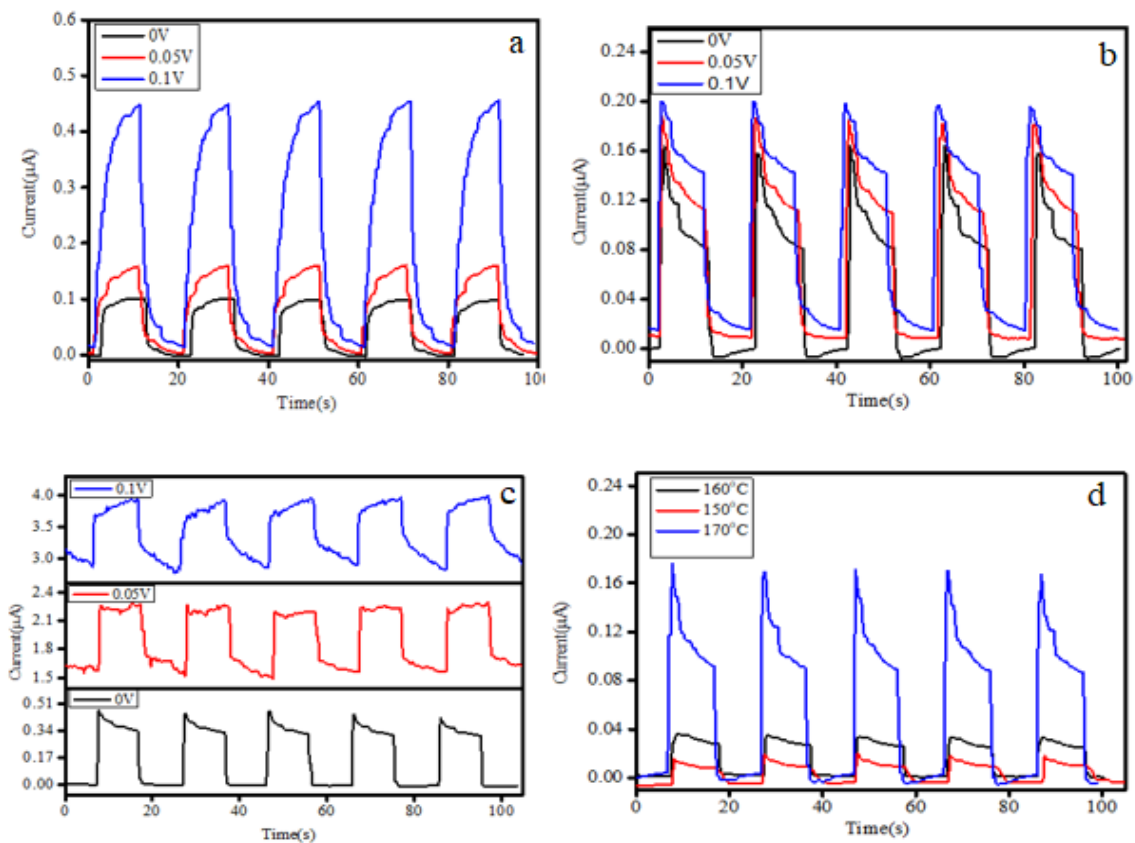


Figure15: Time response (a) of the FTO/TiO<sub>2</sub>/Al reagent prepared at 160°C (b) of the n-TiO<sub>2</sub>/p-SnS<sub>x</sub> reagent (c) of the n-TiO<sub>2</sub>/p-SnO<sub>2</sub> reagent (d) of the n-TiO<sub>2</sub>/p-SnS<sub>x</sub> detector prepared at temperatures (150°C,160°C,170°C) at 0V.

Table 3: Photodetector parameters

Photodetector		$\tau_{\text{rise}}$ (s)	$\tau_{\text{fall}}$ (s)	$I_{\text{light}}$ ( $\mu\text{A}$ )	$I_{\text{dark}}$ ( $\mu\text{A}$ )	$S_{\text{ph}}$ %	R (mA/W)	V (volt)
TiO <sub>2</sub>	160°	1.57	2.70	0.100	0.001	9900	1.98	0
		2.58	3.75	0.158	0.003	5166	3.1	0.05
		4.73	2.86	0.446	0.016	2687	8.6	0.1
TiO <sub>2</sub> /SnS <sub>x</sub>	150°	0.4	0.57	0.024	0.001	2300	0.46	0
		0.56	0.77	0.03	0.002	1400	0.56	0.05
		0.57	0.92	0.036	0.003	1100	0.66	0.1
TiO <sub>2</sub> /SnS <sub>x</sub>	160°	0.18	0.75	0.042	0.011	250	0.62	0
		0.19	0.31	0.059	0.018	227	0.82	0.05
		0.194	0.316	0.081	0.027	200	1.08	0.1
TiO <sub>2</sub> /SnS <sub>x</sub>	170°	0.17	0.32	0.162	0.0004	40400	3.23	0
		0.179	0.53	0.184	0.008	2200	3.52	0.05
		0.21	0.98	0.199	0.015	1226	3.68	0.1
TiO <sub>2</sub> /SnO <sub>2</sub>	160°	0.61	1.36	0.034	0.009	277	0.5	0
		0.4	0.8	19.09	16.02	19	61	0.05
		0.8	1.13	39.3	33.9	15	108	0.1



## Conclusions

XRD assays showed that the shape of the  $\text{TiO}_2$  compound is a tetra-rutile type in all samples and has a preferred growth direction towards (101). We note that when the temperature increases, the intensity of the peaks decreases. The XRD tests confirmed that the samples prepared by the SILAR method that the compound  $\text{SnS}_x$  consists of the two compounds SnS and  $\text{SnS}_2$ , as the shape of the compound SnS is a structure The rhombic compound  $\text{SnS}_2$  has a hexagonal shape. The FE-SEM surface tests showed that the  $\text{TiO}_2$  films are rod-shaped and the upper surfaces are square and perpendicular to the FTO substrate. The optical results of the films of the compound  $\text{SnS}_x$  prepared by the SILAR method showed that the energy gap increases when annealing at a temperature of  $400^\circ\text{C}$  and turns into the compound  $\text{SnO}_2$ . The highest sensitivity is 40400% for the FTO/n- $\text{TiO}_2$ /p- $\text{SnS}_x$ /Al detector with a voltage of 0 V and a rise time of 0.17s with a drop time of 0.3s. Also, the sensitivity decreases with the increase in the applied voltage and its response is fast. We note that the best reagent is FTO/n- $\text{TiO}_2$ /p- $\text{SnS}_x$ /Al.

## References

- [1] M.T. Dhahir, T.A. Salman, Electron Transport Through Two Branch Interferometer with Rashba Spin Orbit Interaction, Bas. J Sci., 39 (2021) 398-413, <https://doi.org/10.29072/basjs.2021305>
- [2] G. Wang, Nanotechnology: The New Features, arXiv preprint arXiv: 1812 (2018) <https://doi.org/10.48550/arXiv.1812.04939>.
- [3] V. Balzani, Nanoscience and Nanotechnology: A Personal View of a Chemist, Small, 1 (2005) 278-283. <https://doi.org/10.1002/sml.200400010>.
- [4] E. Monroy, F. omn`es, F. Calle., Wide-bandgap semiconductor ultraviolet photodetectors, Semicond. Sci. Technol., 18 (2003)R33, <https://doi.org/10.1088/0268-1242/18/4/201>.
- [5] M.J. Kadhim, M.A. Mahdi , J.J. Hassan, Influence of pH on the photocatalytic activity of ZnO nanorods, Materl. Int., ,2(2020) 0064-0072. <https://doi.org/10.33263/Materials21.064072>.
- [6] Assel A Abdul-Hameed, MA Mahdi, Basil Ali, Abbas M Selman, HF Al-Taay, P Jennings, Wen-Jen Lee, Fabrication of a high sensitivity and fast response self-powered photosensor



- based on a core-shell silicon nanowire homojunction, Superlattices and Microstructures, 116(2018) 27-35, <https://doi.org/10.1016/j.spmi.2018.02.003>
- [7] D. J. Mowbray, J. I. Martínez, F. Calle-Vallejo, J. Rossmeisl, K. S. Thygesen, K. W. Jacobsen, J. K. Nørskov, Trends in Metal Oxide Stability for Nanorods, Nanotubes, and Surfaces, The journal of physical chemistry. 115 (2011) 2244-2252. <https://doi.org/10.1021/jp110489u>.
- [8] Y. Shan, Y. Li, H. Pang, Applications of Tin Sulfide-Based Materials in Lithium-Ion Batteries and Sodium-Ion Batteries, Advanced Functional Materials .30 (2020) 2001298. <https://doi.org/10.1002/adfm.202001298> .
- [9] K. Ramasamy, V. Kuznetsov, K. Gopal, M. Malik, J. Raftery, P. Edwards, P. Brien, Organotin Dithiocarbamates: Single-Source Precursors for Tin Sulfide Thin Films by Aerosol-Assisted Chemical Vapor Deposition (AACVD), Chemistry of Materials. 25 (2013): 266-276. <https://doi.org/10.1021/cm301660n>.
- [10] X. Goua, J. Chena, P. Shen, Synthesis, characterization and application of SnS<sub>x</sub> (x = 1, 2) nanoparticles, Materials Chemistry and Physics .93 (2005) 557-566. <https://doi.org/10.1016/j.matchemphys.2005.04.008>.
- [11] MA Mahdi, A Hmood, A Kadhim, JJ Hassan, SJ Kasim, Z Hassan, Solvothermal preparation and characterization of ternary alloy CdS<sub>x</sub>Se<sub>1-x</sub> nanowires, Optik, 127(2016) 1962-1966, <https://doi.org/10.1016/j.ijleo.2015.11.021>
- [12] Y. X. Gan , A. H. Jayatissa, Z. Yu, X. Chen , M. L Department, Hydrothermal Synthesis of Nanomaterials, Journal of Nanomaterials, (2020). <https://doi.org/10.1155/2020/8917013>.
- [13] B. Liu, E. Enache, E. Aydil, Growth of Oriented single-crystalline rutile TiO<sub>2</sub> nanorods on transparent conducting substrates for dye-sensitized solar cells, Journal of the American Chemical Society .131 (2009) 3985-3990. <https://doi.org/10.1021/ja8078972>.
- [14] D. Lee, Q. Xia, R. Mane, J. Yun, K. Kim, Direct successive ionic layer adsorption and reaction (SILAR) synthesis of nickel and cobalt hydroxide composites for supercapacitor applications, J Alloys Comp., 722 (2017) 809-817. <https://doi.org/10.1016/j.jallcom.2017.06.170>
- [15] H . Pathan. C. Lokhande, Deposition of metal chalcogenide thin films by successive ionic



- layer adsorption and reaction (SILAR) method, Bulletin of Materials Science. 27 (2004) 85-111. <https://doi.org/10.1007/BF02708491>.
- [16] Z. H. Nasser, S. J. Kasim, W. S. Hanoosh, Growth, Single-Crystalline Rutile TiO<sub>2</sub> Nanorod Thin Film By Hydrothermal Technique, Basrah university Journal of Kufa-Physics .10 (2018)39–47, <http://dx.doi.org/10.31257/2018/JKP/100206>.
- [17] C. Cao, C. Hu, X. Wang, S. Wang, Y. Tian, H. Zhang, UV sensor based on TiO<sub>2</sub> nanorod arrays on FTO thin film, Sensors and Actuators B: Chemical., 156 (2011) 114-119. <https://doi.org/10.1016/j.snb.2011.03.080>.
- [18] S. Shi, Y. Gao, J. Xu, Influence of electrode materials (Ag, Au) on NiO/TiO<sub>2</sub> heterojunction UV photodetectors, Optik (Stuttg). 224 (2020) 165705. <https://doi.org/10.1016/j.ijleo.2020.165705> .
- [19] Y. Gao, J. Xu, S. Shi, H. Dong, Y. Cheng, C. Wei, X. Zhang, S. Yin, L. Li, TiO<sub>2</sub> Nanorod Arrays Based Self-Powered UV Photodetector: Heterojunction with NiO Nanoflakes and Enhanced UV Photoresponse, ACS applied materials & interfaces .10 (2018): 11269-11279. <https://doi.org/10.1021/acsami.7b18815>.
- [20] J. Chen, J. Xu, S. Shi, R. Cao, D. Liu, Y. Bu, P. Yang, J. Xu, X. Zhang, . L. Li, Novel Self-Powered Photodetector with Binary Photoswitching Based on SnS<sub>x</sub>/TiO<sub>2</sub> Heterojunctions, ACS Appl. Mater. Interf., 12 (2020): 23145-23154. <https://doi.org/10.1021/acsami.0c05247> .
- [21] X. Zu, H. Wang, G. Yi, Z. Zhang, X. Jiang, J. Gong, H. Luo, Self-powered UV photodetector based on heterostructured TiO<sub>2</sub> nanowire arrays and polyaniline nanoflower arrays, Synth. Met., 200 (2015) 58-65. <https://doi.org/10.1016/j.synthmet.2014.12.030> .
- [22] A. Joseph, C. R. Anjitha, A. Aravind, P. M. Aneesh, Applied Surface Science Structural , optical and magnetic properties of SnS<sub>2</sub> nanoparticles and photo response characteristics of p-Si / n-SnS<sub>2</sub> heterojunction diode, Appl. Surf. Sci., 528 (2020) 146977. <https://doi.org/10.1016/j.apsusc.2020.146977>.
- [23] B. R. Sankapal, R. S. Mane, C. D. Lokhande, Successive ionic layer adsorption and reaction (SILAR) method for the deposition of large area (~ 10 cm<sup>2</sup>) tin disulfide (SnS<sub>2</sub>) thin films, Mat. Res. Bull., 35(2000) 2027-2035. [https://doi.org/10.1016/S0025-5408\(00\)00405-0](https://doi.org/10.1016/S0025-5408(00)00405-0).



- [24] M. Rajabi, S. Shogh, A. Iraj, Defect study of TiO<sub>2</sub> nanorods grown by a hydrothermal method through photoluminescence spectroscopy, *Journal of Luminescence*. 157 (2015) 235-242. <https://doi.org/10.1016/j.jlumin.2014.08.035>.
- [25] M. Vishwas, K. N. Rao, R. P. S. Chakradhar, Influence of annealing temperature on Raman and photoluminescence spectra of electron beam evaporated TiO<sub>2</sub> thin films, *Spectrochimica Acta Part A: Mol. Biomol. Spectroscopy*, 99 (2012) 33-36. <https://doi.org/10.1016/j.saa.2012.09.009>.
- [26] M. A. Sinthiya, N. Kumaresan, K. Ramamurthi, K. Sethuraman, M. Babu, R. Babu, Influence of heat treatment on the properties of hydrothermally grown 3D/1D TiO<sub>2</sub> hierarchical hybrid microarchitectures over TiO<sub>2</sub> seeded FTO substrates, *Appl. Surf. Sci.*, 449 (2018) 122-131. <https://doi.org/10.1016/j.apsusc.2018.01.122>.
- [27] Z. Hosseini, M. Shasti, S. Sani, A. Mortezaali, Photo-detector diode based on thermally oxidized TiO<sub>2</sub> nanostructures/p-Si heterojunction, *J Appl. Phys.*, 119 (2016) 014503. <https://doi.org/10.1063/1.4937546>.
- [28] D. Chen, L. Wei, L. Meng, D. Wang, Y. Chen, Y. Tian, S. Yan, L. Mei, J. Jiao, High-Performance Self-Powered UV Detector Based on SnO<sub>2</sub>-TiO<sub>2</sub> Nanomace Arrays, *Nanosc. Res. Lett.*, 13 (2018) 1-7. <https://doi.org/10.1186/s11671-018-2501-x>.



## تحضير ودراسة خصائص اغشية $\text{TiO}_2$ ، $\text{SnS}_x$ و $\text{SnO}_2$ واستعمالها ككواشف للاشعة فوق البنفسجية

نور حسن بدر ، ستار جبار قاسم

قسم الفيزياء، كلية العلوم، جامعة البصرة

### المستخلص

في هذا البحث تم استخدام طريقه Hydrothermal في تحضير اغشية  $\text{TiO}_2$  بدرجات حرارة  $(150,160,170,180)^\circ\text{C}$  مع ثبوت الوقت 6h وطريقة SILAR في تحضير غشاء  $\text{SnS}_x$ . ومن خلال فحوصات XRD يكون شكل المركب  $\text{TiO}_2$  رباعي نوع Rutile بكل العينات وذو اتجاه نمو مفضل باتجاه (101) ونلاحظ عند زيادة درجة الحرارة تقل شدة القمم واما من ناحية التركيز نلاحظ النمو المفضل يكون باتجاه (002) أي عند زيادة التركيز تزداد شدة القمم. اكدت فحوصات XRD ان العينات المحضرة بطريقه SILAR ان المركب  $\text{SnS}_x$  يتكون من المركبين  $\text{SnS}, \text{SnS}_2$  اذ يكون شكل المركب  $\text{SnS}$  هيكل معيني والمركب  $\text{SnS}_2$  يكون شكله سداسي. نلاحظ جميع الكواشف  $\text{Al-TiO}_2, \text{TiO}_2/\text{SnS}_x, \text{TiO}_2/\text{SnO}_2$  الضوئية المصنعة لها سلوك لا خطي شوتكي. ان الكواشف  $\text{Al-TiO}_2$  بدرجات حرارة مختلفة تمتلك حساسية عالية هي حوالي 9900% وتقل حساسية الكاشف بزيادة الجهد المسلط، وذات استجابة بطيئة وبذلك نقوم بتشويبها بالمواد  $\text{SnS}_x, \text{SnO}_2$ . اما في الكواشف  $\text{TiO}_2/\text{SnS}_x, \text{TiO}_2/\text{SnO}_2$  نلاحظ ان اعلى حساسية تكون 40400% عند درجة الحرارة  $160^\circ\text{C}$  وبجهد 0 V وكذلك تقل الحساسية بزيادة الجهد المسلط وتكون استجابته سريعة.

